

Cross sections for ionization and fragmentation of C₆₀ by fast H⁺ impact

H Tsuchida[‡]§, A Itoh[†]||, Y Nakai[‡], K Miyabe[†] and N Imanishi[†]

[†] Department of Nuclear Engineering, Kyoto University, Kyoto 606-8501, Japan

[‡] The Institute of Physical and Chemical Research (RIKEN), Wako 351-0198, Japan

Received 29 May 1998

Abstract. Absolute cross sections have been measured for the first time for H⁺-impact ionization and fragmentation of C₆₀ at proton energies ranging from 0.2 to 2.0 MeV. The cross sections were in fairly good agreement with other electron-impact data in the high-velocity region, indicating that the charge transfer is negligible in the present energy range. Theoretical cross sections for plasmon excitations were also calculated and compared with the experimental ionization cross sections. Agreement between them was within a factor of two, indicating that the plasmon excitation contributes to the total ionization by about 50%. A careful analysis of the energy dependence of the cross sections for C₆₀^{q+} and C_{58,56}^{(q-1)+} ions indicates that these ions are produced from the same initial excited states C₆₀^{*} created in collisions with H⁺ ions.

1. Introduction

In the past numerous experimental studies have been performed on ionization and fragmentation of C₆₀ molecules by using various methods such as photoabsorption [1–5], charged particle impact (electrons [6–11], ions [12–15]) or C₆₀^{1~2+} impact on gaseous targets [16–18]. This is mainly due to its fundamental and practical importance in many areas of physics, chemistry and materials science. In fact, information about various electronic properties of C₆₀, such as ionization or appearance energies of various fragment ions [1, 10, 11], electron energy-loss functions [8], has been accumulated in photoabsorption and electron-impact experiments. In ion-impact experiments particular efforts have been devoted to collision dynamics involving multiple-electron processes such as electron capture as well as ionization and fragmentation. However, few quantitative investigations of cross sections for collision-induced ionization and fragmentation have been carried out [6, 7, 13], and the mechanisms leading to multiple ionization and fragmentation have not yet been understood completely.

Recently, a giant plasmon excitation of C₆₀ received considerable attention in studies of ionization and fragmentation mechanisms. The giant plasmon resonance was first predicted by Bertsch *et al* [19] from the linear-response theory to occur at an excitation energy of about 20 eV with a FWHM of about 10 eV. Experimentally, this plasmon excitation of C₆₀ in the gas phase was first observed by Hertel *et al* [2] using the SR-photoabsorption technique, and by Keller and Coplan [8] using electron energy-loss spectroscopy. In the photoabsorption experiment with photon energies 6–35 eV [2], singly ionized C₆₀⁺ ions

§ Department of Physics, Nara Women's University, Nara 630-8506, Japan

|| Author to whom correspondence should be addressed. E-mail address: itoh@nucleng.kyoto-u.ac.jp

were strongly observed at photon energies corresponding to the giant plasmon excitation, while no other ions originating from multiple ionization or fragmentation were observed. On the other hand, Drewello *et al* [3] observed strong production of triply ionized C_{60}^{3+} ions and doubly charged fragment ions $C_{58,56}^{2+}$ at photon energies above 65 eV, and they claimed that the plasmon excitation enhanced the double and triple ionization. Also, Aksela *et al* [4] stated that C 1s photoelectrons can, with high probability, create the C_{60} plasmon excitation resulting in strong enhancement of singly charged daughter ions. In multiple photoabsorption, Hunsche *et al* [5] pointed out a strong coupling of the plasmon to ionization and fragmentation modes, and stated that the production of C_{60}^{2+} ions and singly charged daughter ions C_{60-2m}^{+} requires at least double-plasmon excitations.

In contrast to these photoabsorption studies, ion-impact experiments relevant to the plasmon excitation have scarcely been performed so far. Using 420–625 MeV $Xe^{18+,35+}$ ions, LeBrun *et al* [13] measured single-ionization cross sections and the results were successfully interpreted within the framework of the single-plasmon excitation model. To obtain further information about the relationship between plasmon excitation and ionization/fragmentation, we used the simplest projectile ion H^+ and measured the absolute cross sections for ionization and fragmentation in the energy range from 0.2 to 2.0 MeV. Cross sections for plasmon excitations were also calculated using the model developed in [13], and discussion about the C_{60} fragmentation mechanism is given.

2. Experimental method

The experimental set-up is essentially the same as that described in our previous paper [15]. Briefly, a H^+ beam from a 1.7 MV tandem Cockcroft–Walton accelerator at Kyoto University was converted into a pulsed beam of about 50 ns width and 10 kHz repetition rate by an electrostatic beam chopping system. The incident beam was carefully collimated to about $2 \times 2 \text{ mm}^2$ with two sets of four-jaw slits before colliding with a C_{60} vapour target in a crossed-beam collision chamber. The beam current was measured with a Faraday cup after the chamber. The vapour target was formed from high-purity (99.98%) C_{60} powder heated to 450 °C in a quartz oven located at the base of the chamber. The powder was initially baked at 250 °C for about 3 days in the chamber at a base pressure of below 1.3×10^{-5} Pa. The oven had an orifice of 2 mm in diameter, through which an effusive C_{60} molecular beam was introduced upward into the collision region. The position of the orifice was about 33 mm below the beam axis. A time-of-flight spectrometer (Wiley–McLaren type [21]) was located perpendicularly both to the H^+ beam and the target beam directions. Extraction of the positively charged fragment ions into the TOF spectrometer was made by applying ± 250 V to two Mo-mesh grids separated by 40 mm. Note that the H^+ beam passed through the centre of these grids. The size of these grids was 60 and 50 mm in the horizontal (beam axis) and in the vertical directions, respectively. The extracted ions were accelerated within a 15 mm gap and then entered a field-free flight tube of 162 mm length. The ion detector was a two-stage (chevron-configuration) multichannel plate with effective detection diameter of 40 mm. The TOF spectra of the fragment ions were obtained by a fast-multichannel scaler (FMCS) with time resolution of 8 ns/channel in 4096 total channels. The start pulse to the FMCS was provided by the beam-chopping control system.

Cross sections for the production of C_n^{q+} ions can be expressed by

$$\sigma_n^{q+} = \frac{Y_n^{q+}}{I_0 N_t L f_M f_c} \quad (2.1)$$

where Y_n^{q+} is the peak intensity of the relevant ions, I_0 the incident beam flux, N_t the number

density of the target molecules, f_c the transmission efficiency of the TOF spectrometer, f_M the MCP detection efficiency and L ($=40$ mm) the collision length, taken to be equal to the MCP detection size. The transmission efficiency f_c represents the ion-arrival rate at the MCP front plate, and depends upon the total transmission of grids, initial kinetic energies and emission angles of the ions. Using the method described in our paper [15], initial kinetic energies of the relevant ions were deduced, and the results were substantially small, of the order 0.05 eV. As described in [15] nearly 100% of such low-energy ions can, independently of their emission angles, be extracted parallel with the spectrometer axis by the extraction field of 125 V cm^{-1} used in the present experiment. Therefore, the loss of ions due to the emission angle could be neglected. On the other hand, there are three grids before reaching the detector. Each grid has a transmission rate of 82%, giving rise to 55% in total. We used this value (0.55) as the transmission efficiency f_c . As for the MCP detection efficiency, Walch *et al* [12] reported the relative efficiencies for C₆₀^{q+} ions; 0.36 ($q = 1$), 0.81 ($q = 2$) and unity ($q \geq 3$) at the MCP front bias of -4.2 kV. In the present work the MCP front bias was -4.9 kV, so that the relative efficiency was estimated to be 0.45 ($q = 1$), 0.89 ($q = 2$) and unity ($q = 3, 4$). The detection efficiency f_M was determined by multiplying these values by an open-area ratio (0.57) of the MCP. The target density N_t of C₆₀ in the collision region was obtained from the vapour pressure data reported by Abrefah *et al* [20] by taking the present experimental geometry into consideration. The target pressure averaged over the collision length L was about 4.3×10^{-5} Pa with a vapour pressure of 1.7×10^{-2} Pa inside the oven at 450°C [20]. Thus we obtained $N_t = 1.05 \times 10^{10} \text{ cm}^{-3}$. Overall experimental errors associated with the cross section measurements were about 20%.

3. Results and discussion

Figure 1 shows a time-of-flight mass distribution of fragment ions produced in collisions between 0.4 MeV H⁺ ions and C₆₀ molecules. Peaks corresponding to multiply charged parent ions C₆₀^{q+} and daughter ions C_{60-2m}^{q+} resulting from even numbered C_{2m} emission were clearly resolved up to $q = 4$. The overall peak structure of these ions is fairly narrow and symmetric in shape, indicating that the formation of these ions is prompt and delayed processes such as electron emission or sequential C₂ loss are insignificant in the present experiment. Furthermore, the initial kinetic energies of these ions obtained from the peak-profile analysis [15] were found to be much smaller than 1 eV as mentioned in the previous section. In the small-mass region one can see only the peaks attributable to residual gases, and small fragment ions such as C₁⁺ or C₂⁺ are nearly absent. This distribution pattern is completely different from those obtained in heavy ion impacts [13–15], where the small fragment ions C_n⁺ ($n \leq 12$), which were produced from C₆₀ multifragmentation, were clearly observed as well as highly charged large fragments. In contrast, the present spectral pattern is similar to those obtained in electron-impact experiments [9, 10]. These experimental findings imply that the nuclear charge Z of projectile particles plays an important role in multifragmentation processes. Namely, if we suppose that the catastrophic decay of C₆₀ molecules occurs only when the projectiles penetrate through the molecules, then the effective charges of the projectiles upon the molecules may increase substantially [22]. Consequently, in the cases of high- Z projectiles large inelastic energies are transferred to the target molecules which eventually become highly excited or multiply ionized. On the other hand, this may not be the case for low- Z projectiles such as protons or electrons.

Absolute cross sections for the production of C_n^{q+} ions ($n = 50\text{--}60$, $q = 1\text{--}4$) are depicted in figure 2. In the following the ionization cross sections $\sigma_q \equiv \sigma_{60}^{q+}$ are discussed first. It is interesting to compare the present ionization cross sections with electron-impact

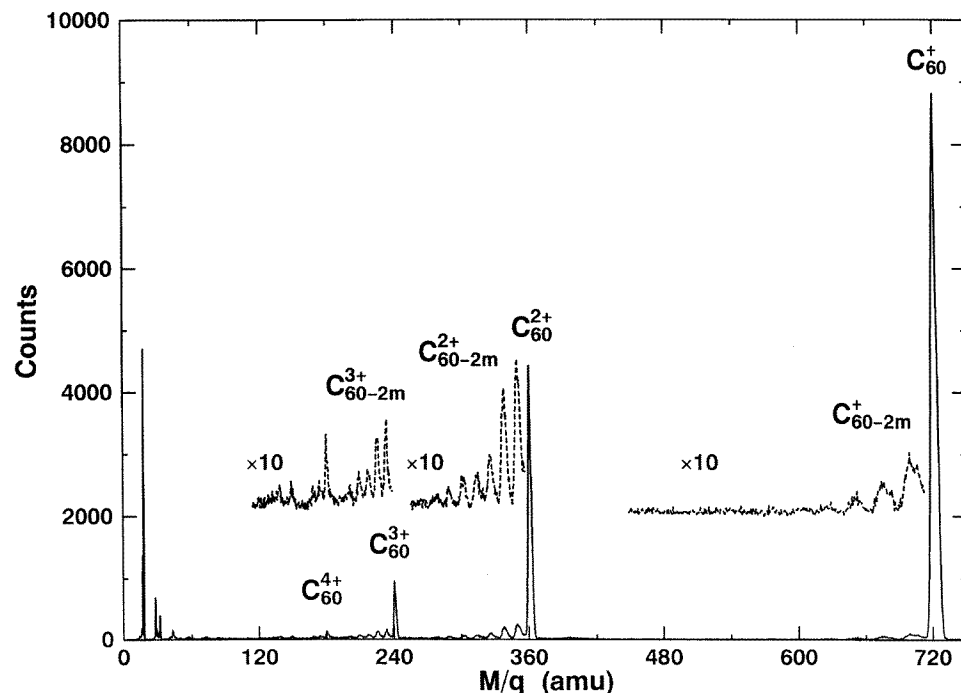


Figure 1. TOF spectra obtained for 0.4 MeV H^+ on a C_{60} vapour target.

data because the formation mechanism of C_{60}^{q+} ions is expected to be different for the two cases. Namely, an electron capture channel is opened in the proton impact case. In figure 3 the cross sections are compared at the same velocities, where the electron-impact data were measured by Dünser *et al* [7] using a two-sector-field mass spectrometer. As can be understood reasonably, the electron-impact ionization cross sections increase rapidly from threshold energies to peak maxima. On the other hand, the present cross sections do not show such an energy dependence, particularly for $q = 3$ and 4. In the high-velocity region the proton- and the electron-impact data show fairly good agreement, indicating that the electron capture process is negligibly small in the present velocity range ($v > 6 \times 10^8$ cm s^{-1}). In both cases the cross sections for $q = 1$ and 2 exhibit extremely broad peak structures. The broad peak structure was also observed for electron-impact ionization of $C_{60}^{1+,2+}$ ions [6]. This is understandable because the measured values are the superposition of individual ionization cross sections of various molecular orbitals with different binding energies or of collective (plasmon) excitations of 240 valence electrons.

To date no rigorous theoretical formalism is available for ion-impact multiple ionization of polyatomic molecules such as C_{60} . LeBrun *et al* [13] developed a plasmon excitation model and successfully applied it for the single ionization of C_{60} by high-energy Xe^{35+} ions. In this model the bound electrons of C_{60} are treated as a free-electron gas and the plasmon excitation is described in terms of a harmonic oscillator with a characteristic frequency ω . An energy transfer $\Delta\epsilon$ from a projectile ion with charge Z_1e and velocity v to a C_{60} molecule is calculated by the dipole approximation [23] in the following expression:

$$\Delta\epsilon = \frac{2Z_1^2e^4}{mv^2} \frac{1}{b^2} \left[\xi^2 K_1^2(\xi) + \frac{1}{\gamma^2} \xi^2 K_0^2(\xi) \right] \quad (3.1)$$

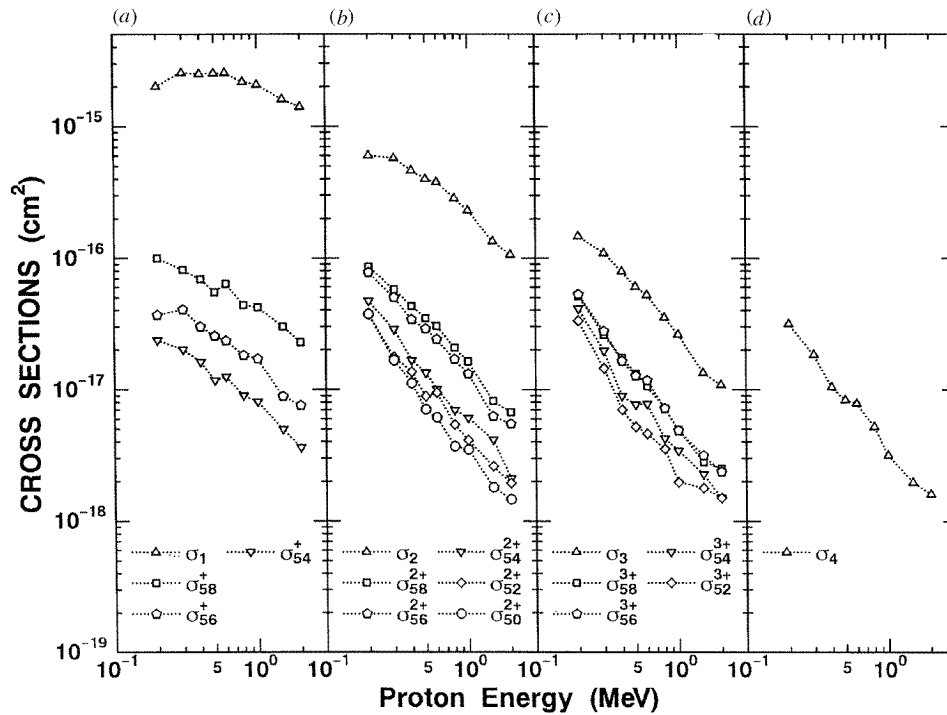


Figure 2. Cross sections for the production of singly to quadruply charged parent ions and daughter ions for $H^+ + C_{60}$ collisions in the energy range of 0.2–2.0 MeV.

where $\xi = Eb/\gamma\hbar v$, $E = \hbar\omega$, K_0 and K_1 are modified Bessel functions of zeroth and first order, respectively, and b is the distance of the beam path from the centre of the molecule. The $\Delta\epsilon$ is spent for the excitation of a giant plasmon with the oscillator strength distribution $f(E)$. The effective number of plasmon excitations $N(b)$ is given by

$$N(b) = \int_0^\infty dE \frac{f(E)}{E} \Delta\epsilon. \tag{3.2}$$

The oscillator strength distribution $f(E)$ is approximated as a Gaussian with known parameters calculated by Bertsch *et al* [19],

$$f(E) = \frac{71}{\sqrt{2\pi} \lambda} \exp\left[-\frac{(E - 20)^2}{2\lambda^2}\right] \tag{3.3}$$

with $\lambda = 10/2.35$ eV. The probability of n -plasmon excitations is given by the Poisson statistics,

$$P_n(b) = \frac{[N(b)]^n}{n!} \exp[-N(b)]. \tag{3.4}$$

Finally, the cross section for n -plasmon excitations is obtained by

$$\sigma_n(\text{pl}) = 2\pi \int b db P_n(b). \tag{3.5}$$

As suggested in [13] the plasmon excitation model is essentially a perturbation theory and it is valid only for distant collisions accompanying small momentum and energy transfer. In the present paper our calculations were performed for $n = 1$ and 2. Calculated results for

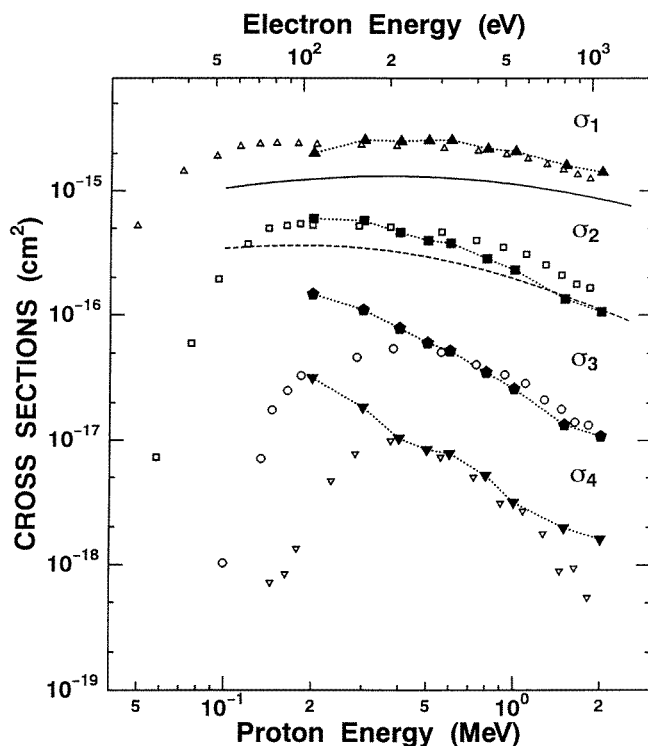


Figure 3. Single- to quadruple-ionization cross sections of C_{60} by H^+ impact (full symbols). Electron-impact ionization cross sections (open symbols) are taken from [7]. The curves represent the theoretical cross sections for plasmon excitations (see text).

single- and double-plasmon excitations are compared in figure 3 with the experimental ionization cross sections σ_1 and σ_2 . As a whole, agreement between theoretical and experimental values are within a factor of two. In 420–625 MeV Xe^{35+} collisions with C_{60} [13], cross sections for the single-plasmon excitation $\sigma_1(pl)$ were found to agree with single-ionization cross sections σ_1 to within a factor of about 2. Consequently, we conclude that the plasmon excitation contributes to total single ionization by roughly 50%. It is worthwhile emphasizing that the simple plasmon excitation model may be applied qualitatively to the ionization processes of C_{60} by fast ions with completely different mass and charges such as H^+ and Xe^{35+} .

Cross sections for the production of fragment ions C_{60-2m}^{q+} are shown in figure 2. It was found that the cross sections σ_{58}^{1-3+} and σ_{56}^{1-3+} were in fairly good agreement with electron-impact data [7] (not shown in the figure). The distinctive feature of the present cross sections is a remarkable q dependence. Namely, as the q increases the cross sections for daughter ions approach the values of corresponding parent ions and also the cross sections with the same q become identical irrespective of their cluster size. Another characteristic feature to be pointed out is a gap between σ_{56}^{q+} and σ_{54}^{q+} , observed clearly for $q = 2$ and probably also for $q = 3$, indicating that the production mechanism of heavier daughter ions ($m \leq 2$) may be different from lighter ions ($m \geq 3$).

In order to see the present results more clearly, cross section ratios between daughter ions and parent ions are plotted in figures 4 and 5 for the total and the partial fragmentation,

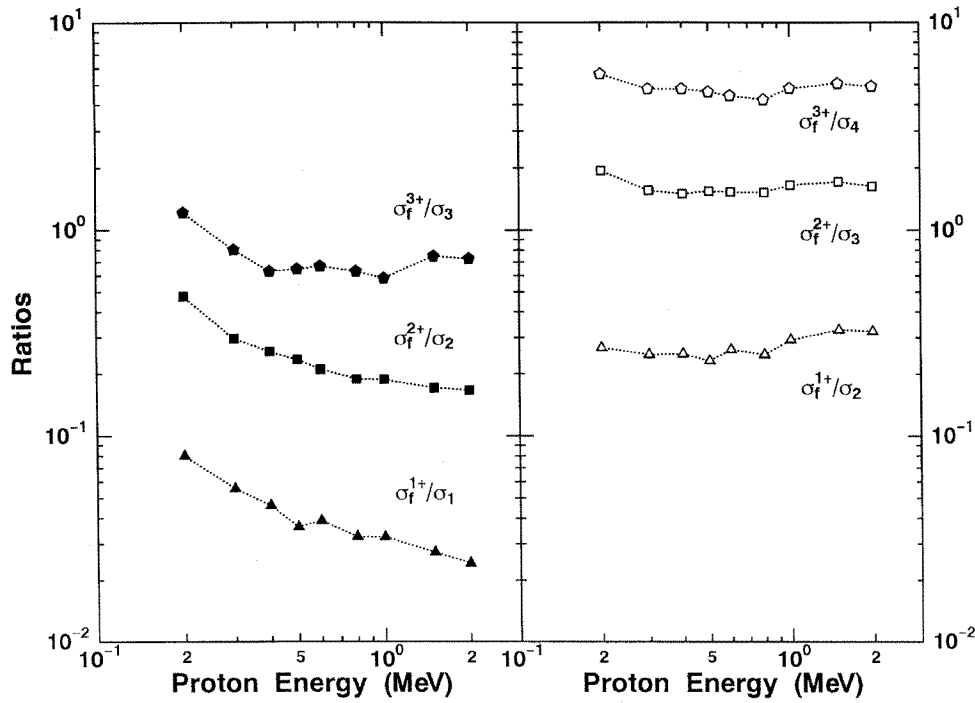
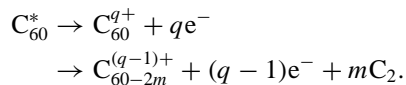


Figure 4. Cross section ratios of total fragmentation to ionization, σ_f^{q+}/σ_q (left-hand side) and $\sigma_f^{(q-1)+}/\sigma_q$ (right-hand side).

respectively. Here, the total fragmentation cross sections σ_f^{q+} denote the sum of cross sections over all daughter ions with the same q . One can see clearly in the left-hand side of figure 4 that the ratios σ_f^{q+}/σ_q are smaller than 0.1 for $q = 1$ but nearly unity for $q = 3$. The most striking feature observed in figure 4 is that the σ_f^{q+}/σ_q exhibit a non-flat energy dependence, while the $\sigma_f^{(q-1)+}/\sigma_q$ shown in the right-hand side are nearly constant. This can be seen more clearly in figure 5, where the partial cross sections $\sigma_{60-2m}^{(q-1)+}/\sigma_q$ for individual fragment ions are shown. The ratios for $m = 1$ and 2 are nearly constant for all q , while for $m \geq 3$ the ratios exhibit non-flat behaviour except for σ_{54}^+ . Hunsch *et al* [5] also found in their photoabsorption experiment a strong correlation between the production of C_{60}^{2+} and C_{60-2m}^+ ions. These results indicate strongly that the ions of C_{60}^{q+} and $C_{60-2m}^{(q-1)+}$ ($m = 1, 2$) may be produced from the same initially excited C_{60}^* molecules via, for instance, the following two decay pathways:



Note that an emission of C_2^+ instead of neutral C_2 in the fragmentation channel may be ruled out because there is no evidence of such ions as demonstrated in figure 1. Since the branching probability for the two pathways may be independent of the incident H^+ energy, it is reasonable to expect the same energy dependence for the production cross sections of $C_{60-2m}^{(q-1)+}$ and C_{60}^{q+} ions.

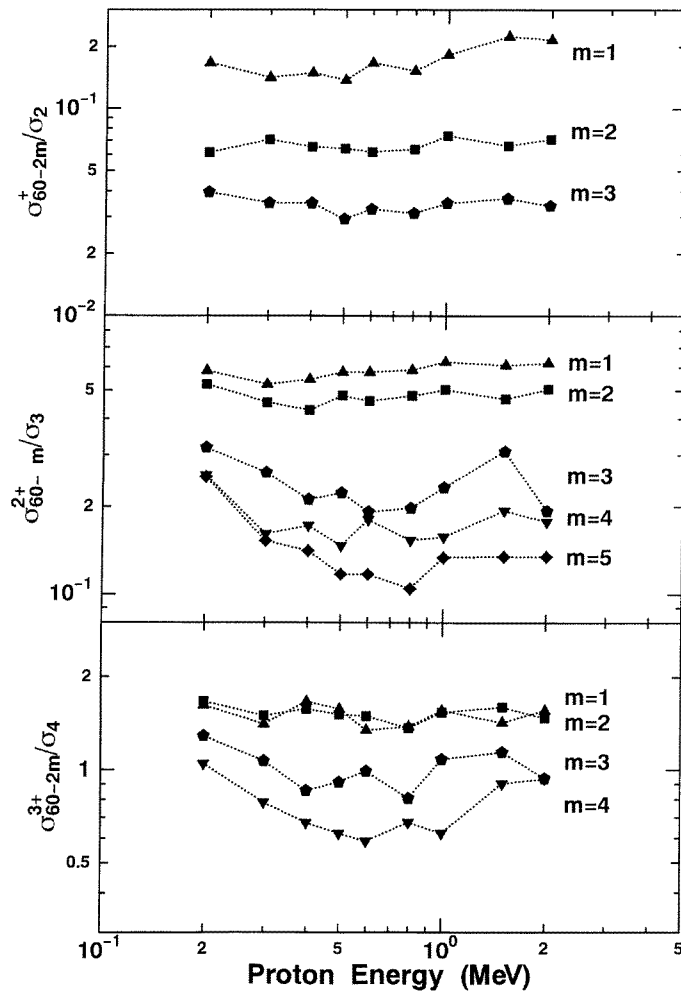


Figure 5. Cross section ratios of partial fragmentation to ionization $\sigma_{60-2m}^{(q-1)+}/\sigma_q$.

4. Conclusions

We have measured the cross sections for proton-impact ionization and fragmentation of C_{60} in the energy range 0.2–2.0 MeV. In this range the electron transfer process was found to be negligibly small and the cross sections were in fairly good agreement with electron-impact data [7]. On the basis of the plasmon excitation model developed by LeBrun *et al* [13] we have calculated cross sections for single- and double-plasmon excitations. The calculated values were in agreement with single- and double-ionization cross sections within a factor of two. This may imply that a contribution from the plasmon excitation to the total ionization of C_{60} is roughly 50%. We found that the cross sections $C_{58,56}^{(q-1)+}$ reveal the same energy dependence as σ_{60}^{q+} , indicating that these ions are produced from the same initially excited states following the decay pathways as proposed in the previous section.

Acknowledgments

We would like to thank M Imai for valuable discussion and K Yoshida and K Norisawa for their technical support during the present experiment.

References

- [1] Yoo R K, Ruscic B and Berkowitz J 1992 *J. Chem. Phys.* **92** 911
- [2] Hertel I V, Steger H, de Vries J, Weisser B, Menzel C, Kamke B and Kamke W 1992 *Phys. Rev. Lett.* **68** 784
- [3] Drewello T, Krättschmer, Erdmann F-M and Ding A 1993 *Int. J. Mass Spectrom. Ion Processes* **124** R1
- [4] Aksela S, Nömmiste E, Jauhiainen J, Kukk E, Karvonen J, Berry H G, Sorensen S L and Aksela H 1995 *Phys. Rev. Lett.* **75** 2112
- [5] Hunsche S, Starczewski T, L'Huillier A, Persson A, Wahlström C-G, van Linden van den Heuvell B and Svanberg S 1996 *Phys. Rev. Lett.* **77** 1966
- [6] Völpel R, Hofmann G, Steidl M, Stenke M, Schlapp M, Trassl R and Salzborn E 1993 *Phys. Rev. Lett.* **71** 3439
- [7] Dünser B, Lezius M, Scheier P, Deutsch H and Märk T D 1995 *Phys. Rev. Lett.* **74** 3364
Matt S, Dünser B, Lezius M, Deutsch H, Becker K, Stamatovic A, Scheier P and Märk T D 1996 *J. Chem. Phys.* **105** 1880
- [8] Keller J W and Coplan M A 1992 *Chem. Phys. Lett.* **22** 89
- [9] Luffer D R and Schram K H 1990 *Rapid Commun. Mass Spectrosc.* **4** 552
- [10] Srivastava S K, Jong G, Leifer S and Saunders W 1993 *Rapid Commun. Mass Spectrosc.* **7** 610
- [11] Wörgötter R, Dünser B, Scheier P and Märk T D 1994 *J. Chem. Phys.* **101** 8674
- [12] Walch B, Cocke C L, Voelpel R and Salzborn E 1994 *Phys. Rev. Lett.* **72** 1439
- [13] LeBrun T, Berry H G, Cheng S, Dunford R W, Esbensen H, Gemmell D S, Kanter E P and Bauer W 1994 *Phys. Rev. Lett.* **72** 3965
Cheng S, Berry H G, Dunford R W, Esbensen H, Gemmell D S, Kanter E P, LeBrun T and Bauer W 1996 *Phys. Rev. A* **54** 3182
- [14] Nakai Y, Itoh A, Kambara T, Bitoh Y and Awaya Y 1997 *J. Phys. B: At. Mol. Opt. Phys.* **30** 3049
- [15] Itoh A, Tsuchida H, Miyabe K, Imai M and Imanishi N 1997 *Nucl. Instrum. Methods B* **129** 363
- [16] Hvelplund P, Andersen L H, Haugen H K, Lindhard J, Lorents D C, Malhotra R and Ruoff R 1992 *Phys. Rev. Lett.* **69** 1915
- [17] Hvelplund P, Andersen L H, Brink C, Yu D H, Lorents D C and Ruoff R 1994 *Z. Phys. D* **30** 323
- [18] Shen H, Hvelplund P, Mathur D, Bárány A, Cederquist H, Selberg N and Lorents D C 1995 *Phys. Rev. A* **52** 3847
- [19] Bertsch G F, Bulgac A, Tománek D and Wang Y 1991 *Phys. Rev. Lett.* **67** 2690
- [20] Abrefah J, Olander D R, Balooch M and Siekhaus W J 1992 *Appl. Phys. Lett.* **60** 1313
- [21] Wiley W C and McLaren I H 1955 *Rev. Sci. Instrum.* **26** 1150
- [22] McGuire J H, Stolterfoht N and Simony P R 1981 *Phys. Rev. A* **24** 97
- [23] Jackson J D 1962 *Classical Electrodynamics* (New York: Wiley)